Journal of the European Ceramic Society 21 (2001) 1967–1970

www.elsevier.com/locate/jeurceramsoc

Ceria-based gas sensors

Todd S. Stefanik, Harry L. Tuller *

Department of Materials Science and Engineering, Crystal Physics and Electroceramics Laboratory, Massachusetts Institute of Technology, Cambridge, MA 02139, USA

Received 4 September 2000; received in revised form 30 November 2000; accepted 5 December 2000

Abstract

The electrical conductivity of $Pr_xCe_{1-x}O_{2-\delta}$ (PCO) with $x \leqslant 0.05$ was examined as functions of praseodymium content (x), oxygen partial pressure and temperature and a defect model based on multiple oxidation states of Pr was found to be consistent with the data. These results are used to examine PCOs potential as an active film in gravimetric sensors. © 2001 Elsevier Science Ltd. All rights reserved.

Keywords: CeO_2; Defects; Electrical conductivity; Sensors

1. Introduction

Monitoring and detection of gases is of importance for emissions, toxic gas detection, and for process control. A number of detection principles have, in the past, been investigated and applied including those based on electrochemical, semiconducting, and calorimetric methods.[1,2] Electroceramics enable operation at elevated temperatures, which is important given that many gas reactions are kinetically hindered under ambient conditions. Another possible method, based on gravimetric principles, is normally limited to or the near vicinity of room temperature. Here, either quartz shear wave resonant transducers or surface acoustic wave (SAW) devices are used to detect gases selectively absorbed, typically on deposited polymer films, by measuring the shift in the resonant frequency of the acoustic wave device. Recently, application temperatures as high as 450°C have been achieved with quartz devices;[3] above this temperature, high losses and phase transitions prevent its use. We have initiated a study of the high temperature properties of langasite, $La_3Ga_5SiO_{14}$, a piezoelectric material stable to temperatures well above 1000°C. Furthermore, we have demonstrated the ability to measure the resonant frequency, ω_0, of a shear wave device utilizing langasite to temperatures above 600°C as well as shifts induced in ω_0 by mass loading.[4,5]

In this study, we investigate materials in the solid solution system $Pr_xCe_{1-x}O_{2-\delta}$ (PCO) which have been shown to exhibit extensive deviations from stoichiometry, δ, and rapid redox kinetics,[6] both characteristics of importance for "active" films to be incorporated into a gravimetric gas sensor. In order to be able to predict the performance of PCO in this application, one must have a defect model describing the dependence of δ and the chemical diffusivity, D_{chem}, on x, Po_2 and temperature. Towards this end, we have initiated electrical conductivity measurements as a function of the three key parameters listed above. To date, except for preliminary reports by one of the authors[7] electrical measurements in the binary system $Pr_xCe_{1-x}O_{2-\delta}$ have been limited to temperature-dependent measurements performed in air or pure oxygen.[8,9] A defect model appropriate for low values of x ($x \leqslant 0.05$) is derived and reported in this paper.

2. Experimental methods

Dense pellets of PCO solid solutions with $x = 0$, 0.001, 0.005, 0.01 and 0.05 were prepared by (1) co-precipitation of Ce and Pr oxalates by reaction of the nitrates with oxalic acid, (2) calcination of the resultant powders at 700°C for 60 min in air, (3) pressing the calcined powders into pellets at 125 MPa without binder, and (4) sintering them at 1425°C for 10 h. XRD analysis confirmed the formation of single phase fluorite. SEM micrographs showed a uniform microstructure with

* Corresponding author. Tel.: +1-617-253-6890; fax: +1-617-258-5749.

E-mail address: hltuller@mit.edu (H.L. Tuller).

PII: S0955-2219(01)00152-2

grain size of ≅5 μm, while measured weight to volume ratios indicated densities of ≅95% of theoretical.

Four point dc electrical conductivity measurements were performed on rectangular-shaped specimens cut out of the ≅1.5 cm diameter pellets. Platinum leads were wrapped around each specimen with Pt paint (Englehard) used to improve the electrical contact between specimen and leads. Six specimens were simultaneously loaded into the sample chamber which included a stabilized zirconia oxygen sensor and thermocouples attached to each individual specimen. Current-voltage sweeps were recorded for each specimen via an HP 34970A data acquision unit interfaced with a computer. Oxygen partial pressures were controlled by the use of CO/CO_2 and Ar/O_2 mixtures with values reported in this work measured by the in situ oxygen sensor.

3. Results and discussion

A series of conductivity isotherms for $Pr_{0.05}Ce_{0.95}O_{2-\delta}$ are shown in Fig. 1 as a function of Po_2. At low and intermediate Po_2 values, the conductivity follows the Po_2 dependence expected for a fixed-valent acceptor doped system, i.e. a pressure- independent ionic regime at intermediate Po_2 followed by a partial pressure-dependent electronic conductivity at low Po_2. At high Po_2, however, the conductivity decreases with increasing Po_2, pointing to the existence of a different defect regime. This, shown below, is related to the oxidation of the Pr^{3+} acceptors to Pr^{4+}, resulting in a region of Po_2-dependent ionic conductivity not observed in fixed-valence acceptor doped systems.

In the following, we describe a defect model which includes a variable valent acceptor dopant such as Pr in PCO. First we note that in the fluorite system, Frenkel defects dominate ionic disorder, resulting in the formation of oxygen vacancies and interstitials:

$$O_O'' \rightarrow V_O^{\cdot\cdot} + O_i'', \qquad [V_O^{\cdot\cdot}][O_i''] = K_F(T) \tag{1}$$

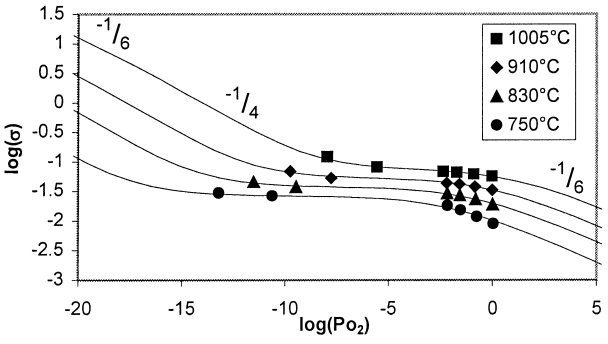

Fig 1. Conductivity as a function of Po_2 in $Pr_{0.05}Ce_{0.95}O_{2-\delta}$. Solid lines are fits to the model described below.

Electronic disorder is governed by the reaction:

$$\text{nil} \rightarrow e' + h^{\cdot}, \qquad np = K_e(T) \tag{2}$$

Reduction of the ceria host occurs via:

$$O_O^X \rightarrow 1/2O_2(g) + V_O^{\cdot\cdot} + 2e', \qquad [V_O^{\cdot\cdot}]n^2 Po_2^{1/2} = K_R(T) \tag{3}$$

In addition, ionization of the Pr^{3+} acceptors must be taken into account:

$$Pr_{Ce}' \rightarrow Pr_{Ce}^X + e', \qquad [Pr_{Ce}^X]n/[Pr_{Ce}'] = K_{Pr}(T) \tag{4}$$

The praseodymium mass balance is given by:

$$Pr_{tot} = [Pr_{Ce}'] + [Pr_{Ce}^X] \tag{5}$$

where Pr_{tot} is the total amount of Pr added in solid solution. Finally, electroneutrality dictates that:

$$2[O_i''] + n + [Pr_{Ce}'] = p + 2[V_O^{\cdot\cdot}] \tag{6}$$

This system of six equations and six unknowns is complex to solve. Noting that praseodymium enhances the reduction of ceria, it is reasonable to assume that the concentrations of oxygen interstitials and holes are negligible relative to the other charged species. Therefore:

$$n + [Pr_{Ce}'] \approx 2[V_O^{\cdot\cdot}] \tag{7}$$

Following the method suggested by Porat and Tuller,[10] one can solve for Po_2 in terms of n yielding:

$$Po_2 = \left[\frac{2K_R}{n^3}\left(\frac{n + K_{Pr}}{n + K_{Pr} + Pr_{tot}}\right)\right]^2 \tag{8}$$

The general characteristics of this model are shown in Fig. 2. There are four regions of conductivity behavior incorporated in the model. In region I, a $Po_2^{-1/6}$ dependence is observed as is expected for reduction-controlled electronic behavior at low Po_2. Region II corresponds to electronic conductivity when the oxygen vacancy concentration is fixed at a constant level by acceptor dopants and exhibits the anticipated $Po_2^{-1/4}$ dependence. In Region III, the vacancy concentration remains set by the acceptors, but the *n*-type electronic drops below the ionic conductivity, resulting in a Po_2 independent behavior. Finally in region IV, oxidation of Pr^{3+} to Pr^{4+} results in a $Po_2^{-1/6}$ dependent oxygen ion conductivity. The solutions for the defects dominating the total conductivity in each region and the approximations used in Eq. (8) to obtain them are summarized in Table 1.

Table 1
Solutions for the dominant defects in each regime of the defect model for $Pr_xCe_{1-x}O_{2-\delta}$

Region I	Region II	Region III	Region IV
$n >> K_{Pr}$ ($[Pr_{Ce}'] >> [Pr_{Ce}^X]$)	$n >> K_{Pr}$ ($[Pr_{Ce}'] >> [Pr_{Ce}^X]$)	$n >> K_{Pr}$ ($[Pr_{Ce}'] >> [Pr_{Ce}^X]$)	$K_{Pr} >> n([Pr_{Ce}^X] >> [Pr_{Ce}'])$
$n >> Pr_{tot}$, $n = 2[V_O^{\cdot\cdot}]$	$Pr_{tot} >> n$, $2[V_O^{\cdot\cdot}] = [Pr_{Ce}']$	$Pr_{tot} >> n$, $2[V_O^{\cdot\cdot}] = [Pr_{Ce}']$	$Pr_{tot} >> K_{Pr}$, $2[V_O^{\cdot\cdot}] = [Pr_{Ce}']$
$\sigma \propto n = (2K_R)^{1/3} Po_2^{-1/6}$	$\sigma \propto n = \frac{(2K_R)^{1/2}}{(Pr_{tot})^{1/2}} Po_2^{-1/4}$	$\sigma \propto 2[V_O^{\cdot\cdot}] = \frac{[Pr_{Ce}']}{2}$	$\sigma \propto [V_O^{\cdot\cdot}] = \frac{K_R^{1/3}}{(2K_{Pr})^{2/3}} Pr_{tot}^{2/3} Po_2^{-1/6}$

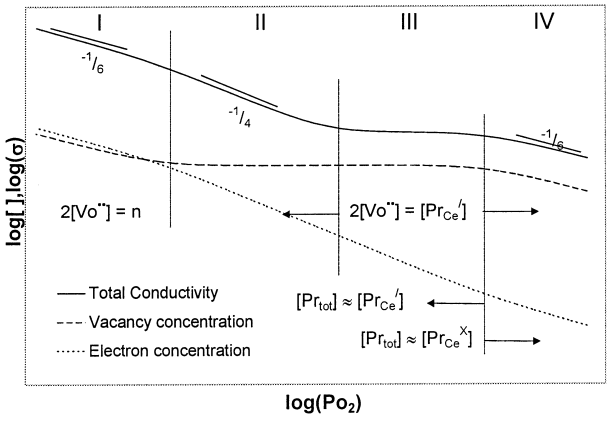

Fig. 2. Concentrations of vacancies and electrons and the total electrical conductivity plotted vs. Po_2 for the four defect regimes.

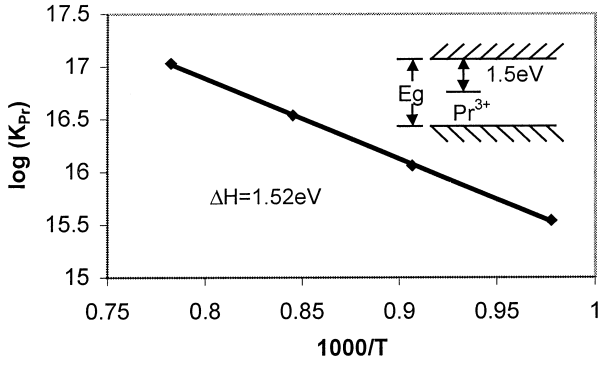

Fig. 3. Temperature variation of the ionization constant K_{Pr} for $x = 0.05$ in PCO.

The following procedure was used to fit our model to the experimental data. At each temperature, the ionic conductivity was extracted from the plateau region of the curve (where the relationship $Pr_{tot} \approx 2[V_O^{\cdot\cdot}]$ applies) and an ionic mobility was calculated based on the conductivity and the calculated vacancy concentration. The mobility values exhibited the expected Arrhenius behavior with an activation energy of 0.46 eV. The values for K_R and the electronic mobility μ_e were taken from studies performed on undoped single crystal ceria[11,12] and are assumed to be unaffected by Pr additions, at least up to the 5% levels examined in this study. Eq. (8) was then fit to the data. Fig. 1 shows that the model fits the data quite well for PCO with $x = 0.05$.

Derived values for $K_{Pr,}$ plotted in Fig. 3 as a function of temperature, follow an Arrhenius behavior with an enthalpy of ionization of 1.52 eV. This indicates that Pr^{3+} forms relatively deep traps in PCO, lying somewhere near mid-gap.

While the data for PCO with $x = 0.05$ fit the model rather well, samples containing lower concentrations of Pr proved more troublesome. This we trace to the increasing importance of background impurities in the raw materials used to prepare the samples. At high doping levels, the effect of Pr^{3+} is sufficient to mask the effects of background impurities. As the doping level approaches the background acceptor level, contributions to the overall conductivity from the two begin to compete with one another. The model was modified to accommodate fixed valence impurities and an analytic solution similar to that for the background impurity-free case was found. However, further experiments are required in order to accurately determine the background acceptor impurity level and calculate the ionization constant for praseodymium in samples with a lower doping level. Likewise, the experiments are being extended to lower pressures to confirm the electron transition to a $Po_2^{-1/6}$ dependence more clearly.

4. Summary and conclusions

The electrical conductivity measurements of PCO with $x \leqslant 0.05$ were examined as functions of Po_2 and T and a defect model based on multiple oxidation states of Pr was found to be consistent with the data. These results confirm that Pr markedly increases the degree of nonstoichiometery in ceria under oxidizing conditions and thereby its potential utility in gravimetric sensors as the active film. Further studies are being pursued to extend the ranges of x, Po_2 and temperature and to establish the rate limiting steps controlling the redox kinetics.

Acknowledgements

This work was supported by the National Science Foundation under the Goali program DMR97-01699 and the International Program INT-98155788. Discussions with H. Fritze and H. Seh are appreciated.

References

1. Hill, D. C. and Tuller, H. L., Ceramic sensors: theory and practice. In *Ceramic Materials for Electronics*, 2nd edn, ed. R. C. Buchanan. Marcel Dekker, NY, 1991, pp. 249–347.
2. Tuller, H. L. and Mlcak, R., Photo-assisted silicon micromachining: opportunities for chemical sensing. *Sensors and Actuators B*, 1996, **35/36**, 255–261.
3. Cernosek, R. W., Bigbie, J. R., Anderson, M. T., Small, H. H. and Sawyer, P. S. High temperature hydrocarbon gas sensing with mesoporous SiO_2 thin films on TSM resonators, solid-state and actuator workshop, Hilton Head Island, S.C. 6/8–11/1998.
4. Fritze, H., Tuller, H. L., Borchardt, G. and Fukuda, T., High temperature properties of langasite. In Symposium on Smart Materials, eds. R. Gotthardt, K. Uchino, Y. Ito, and W. Wun-Fogle, MRS Symposium Proceedings, Vol. 604. Materials Research Society, Warrendale, PA, 2000, pp. 6570.
5. Fritze, H., Tuller, H. L., She, H. and Borchardt, G., High temperature nanobalance sensor based on langasite. *Proc. of Int. Meeting Chemical Sensors*. Basil, Switzerland, July 5, 2000. In press.
6. Knauth, P. and Tuller, H. L., Nonstoichiometry relaxation kinetics of nanocrystalline mixed praseodymium-cerium oxide $Pr_{0.7}Ce_{0.3}O_{2-x}$. *J. Eur. Ceram. Soc.*, 1999, **19**, 831–836.
7. Porat, O., Tuller, H. L., Shelef, M. and Logothetis, E. T., Electrical conductivity and nonstoichiometry in $Pr_{0.545}Ce_{0.455}O_{2-x}$. In *Solid-State Chemistry of Inorganic Materials* (MRS Symp. Vol. 453), ed. P. K. Davies, A. J. Jacobson, C. C. Torardi and T. A. Vanderah. Materials Research Society, Pittsburgh, PA, 1997, pp. 531–535.
8. Shuk, P. and Greenblatt, M., Hydrothermal synthesis and properties of mixed conductors based on $Ce_xPr_{1-x}O_{2-\delta}$ solid solutions. *Solid State Ionics*, 1999, **116**, 217–223.
9. Ftikos, C. and Steele, B. C. H., Electrical Conductivity and Thermal Expansion of Ceria Doped with Pr, Nb, and Sn. *J. Eur. Ceram. Soc.*, 1993, **12**, 267–270.
10. Porat, O. and Tuller, H. L., Simplified analytical treatment of defect equilibria: application to oxides with multi-valent dopants. *J. Electroceramics*, 1997, **1**, 41–49.
11. Tuller, H. L. and Nowick, A. S., Defect structure and electrical properties of nonstoichiometric CeO_2 single crystals. *J. Electrochem. Soc.*, 1979, **126**, 209–217.
12. Tuller, H. L. and Nowick, A. S., Small polaron electron transport in reduced CeO_2 single crystals. *J. Phys. Chem. Solids*, 1977, **38**, 859–867.